

SUV39H1 Inhibits Angiogenesis in Limb Ischemia of Mice

Cell Transplantation
Volume 32: 1–15
© The Author(s) 2023
Article reuse guidelines:
sagepub.com/journals-permissions
DOI: 10.1177/09636897231198167
journals.sagepub.com/home/cll



Wenhao Niu^{1*}, Wenyue Cao^{2*}, Feng Wu³, and Chun Liang¹

Abstract

Peripheral arterial disease (PAD), characterized by atherosclerosis of the peripheral arteries or even amputation, has threatened public life and health. However, the underlying mechanism remains largely obscure. SUV39H1, a histone methyltransferase, could specifically methylate lysine 9 of histone H3 and act as a repressor in transcriptional activity. The study aimed to investigate the role of SUV39H1 in limb ischemia. C57BL/6 male mice were randomly divided into Sham or Model groups to investigate the expression of SUV39H1 in the ischemic limbs. Then, pharmaceutical inhibition or genetic deletion of SUV39H1 in the limb ischemia mice model was performed to confirm its effect on limb ischemia. The blood perfusion was quantified by laser speckle contrast imaging (LSCI). Capillary density and muscle edema were measured by CD31 immunohistochemical staining and HE staining. The expressions of SUV39H1 and Catalase were confirmed by western blot. Transcriptome sequencing of siSUV39H1 in human umbilical vein endothelial cells (HUVECs) was used to explore the regulation mechanism of SUV39H1 on angiogenesis. The results showed that SUV39H1 was highly expressed in the ischemic muscle tissue of the mice. Pharmaceutical inhibition or genetic deletion of SUV39H1 significantly improved blood perfusion, capillary density, and angiogenesis in ischemic muscle tissue. Cell experiments showed that SUV39H1 knockdown promoted cell migration, tube formation, and mitochondrial membrane potential in endothelial cells under oxidative stress. The transcriptome sequencing results unmasked mechanisms of the regulation of angiogenesis induced by SUV39H1. Finally, Salvianolic acid B and Astragaloside IV were identified as potential drug candidates for the improvement of endothelial function by repressing SUV39H1. Our study reveals a new mechanism in limb ischemia. Targeting SUV39H1 could improve endothelial dysfunction and thus prevent limb ischemia.

Keywords

SUV39H1, vascular disease, endothelial dysfunction, limb ischemia

Introduction

Peripheral arterial disease (PAD) is a clinical complication of atherosclerosis that obstructs multiple vascular beds such as lower extremities by embolism or thrombosis leading to amputation or even early death¹. An accurate calculation of the incidence rates of PAD is challenging due to its chronic course and insidious onset; it is estimated that 10% to 20% of the population will eventually suffer from PAD in individuals aged above 60 years^{1–4}.

Hypoxia and oxidative stress could affect protein status during the ischemic period^{5–8}. Thereafter, intracellular proteins undergo various modifications to regulate the damage to tissues and cells. Among diverse modifications, histone methylation is common in ischemic issues^{9,10}. It acts as a regulator in the pathophysiology of the disease process and currently has extensive studies^{10–12}. Previous studies have proposed that trimethylation of histone H3 lysine 4 (H3K4Me3) regulates

¹ Department of Cardiology, Shanghai Changzheng Hospital, Naval Medical University, Shanghai, China

² Department of Ultrasonography, Shanghai Chest Hospital, Shanghai Jiao Tong University School of Medicine, Shanghai, China

³ Department of Cardiology, Yueyang Hospital of Integrated Traditional Chinese and Western Medicine, Shanghai University of Traditional Chinese Medicine, Shanghai, China

*These authors contributed equally to this work.

Submitted: April 11, 2023. Revised: August 7, 2023. Accepted: August 15, 2023.

Corresponding Authors:

Feng Wu, Department of Cardiology, Yueyang Hospital of Integrated Traditional Chinese and Western Medicine, Shanghai University of Traditional Chinese Medicine, Shanghai 200437, China.
Email: wufengmed@163.com

Chun Liang, Department of Cardiology, Shanghai Changzheng Hospital, Naval Medical University, Shanghai 200003, China.
Email: chunliangliang1985@163.com



transcriptional activation, nevertheless, trimethylation of H3 lysine 9 (H3K9Me3) regulates transcriptional repression¹³. SUV39H1, a histone methyltransferase, could specifically methylate lysine 9 of histone H3 and acts as a repressor in transcriptional activity. The previous study showed that SUV39H1 has different roles in different diseases. It modulates the oxidative capacity of vessels and thus prevents vascular disease in the obese adult population¹⁴. Furthermore, SUV39H1 could aggravate cardiac injury following myocardial infarction¹³. However, the direct effects of SUV39H1 on angiogenesis and the pathogenesis of limb ischemia remain largely elusive.

We report here that up-regulation of SUV39H1 during limb ischemia in mice model. Genetic deletion or pharmaceutical inhibition of SUV39H1 alleviated limb ischemia. Moreover, the oxidative stress activated the SUV39H1 expression in endothelial cells, and SUV39H1 knockdown improved tube formation, cell migration, and mitochondrial membrane potential (MMP) under oxidative stress stimulation. Taken together, we provide the rationale for targeting SUV39H1 to treat limb ischemia.

Materials and Methods

Chemicals and Reagents

Chaetocin (purity: 98.66 %, Cat. No. S8068), Salvianolic acid B (Sal B, purity: 99.73%, Cat. No. S4735), and Astragaloside IV (AS-IV, purity: 98%, Cat. No. S3901) were obtained from Selleck (Houston, TX, USA). CD31 immunohistochemical staining antibody was purchased from Cell Signaling Technology (Danvers, MA, USA). Antibodies to SUV39H1, Catalase, and glyceraldehyde 3-phosphate dehydrogenase (GAPDH) were purchased from ProteinTech Wuhan Sanying Biotechnology (Wuhan, China). RIPA lysis buffer, PMSF, and protease inhibitor cocktail were obtained from Beyotime Biotechnology (Shanghai, China), a BCA Protein Assay Kit was bought from Thermo Fisher Scientific (Carlsbad, CA, USA), secondary antibody was obtained from Abcam (Cambridge, United Kingdom), and ECL reagent was brought from Advansta (CA, USA). RNAiso and PrimeScript RT Master Mix were brought from TaKaRa (TaKaRa, Tokyo, Japan), and SYBR Green PCR Kit was purchased from Vazyme (Nanjing, China). Endothelial cell medium (ECM) and endothelial cell growth supplement (ECGS) were brought from Sciencell (CA, USA). Matrigel matrix was brought from Corning (MA, USA). Transwell chambers (8 μ m) were brought from Corning (NY, USA). HiPerFect transfecting reagent was purchased from Qiagen (Hilden, Germany). Lipofectamine 3000 was obtained from Invitrogen (CA, USA). The JC-1 probe mitochondrial membrane potential detection kit was brought from Beyotime (Shanghai, China). Hydrogen peroxide (H₂O₂, 30%) was obtained from Merck. Human recombinant SUV39H1 protein was purchased from Huanqiu Jiyin Science and

Technology Co. Ltd. (Anhui, China). Series CM5 sensor chip was obtained from GE Life (USA).

Animals

Male C57BL/6J mice, 5 weeks old, were purchased from Ji Hui Experimental Animal Breeding Company (Shanghai, China). SUV39H1 knockout mice aged 5 weeks were obtained from Professor Aijun Sun (Shanghai Institute of Cardiovascular Disease, Zhongshan Hospital, Fudan University, Shanghai 200032, China; Institute of Biomedical Sciences, Fudan University, Shanghai 200032, China). Animals were housed in a room with a 12: 12-h light/dark cycle and free access to food and drinking water in the Animal Center of Naval Medical University. All of the experimental procedures were approved by the Ethics Review of Animal Use Application of Naval Medical University (license number SYXK [HU] 2017-004). All procedures were performed following the National Institutes of Health Guide for the Care and Use of Laboratory Animals. All operations were performed under anesthesia, and all possible efforts were taken to minimize suffering in accordance with the ARRIVE guidelines on animal research.

Establishment of Hind Limb Ischemia Model and Intraperitoneal Administration

Model mice were anesthetized by sodium pentobarbital intraperitoneally (60 mg/kg body weight). The establishment of the hind limb ischemia model was described in a previous study¹⁵. To explore the effect of chaetocin, a specific inhibitor of SUV39H1, on the improvement of limb ischemia, model mice were randomly assigned to either a Model + DMSO group or a Model + Chaetocin group (0.25 mg/kg) for 12 d before the mice were sacrificed. The injection of chaetocin was delivered intraperitoneally. To further verify the effect of SUV39H1 on the improvement of limb ischemia, a group of SUV39H1 knockout mice underwent limb ischemia surgery as well.

Laser Speckle Contrast Imaging

The laser speckle contrast imaging (LSCI) system (Perimed Instruments AB, Sweden) was used before, immediately after, and on Days 4, 8, 12, 14, and 16 after the operation. The blood flow recovery ratio = ischemic limb perfusion (left hind limb)/nonischemic limb perfusion (right hind limb) \times 100%.

HE Staining and CD31 Immunohistochemical Staining

On the endpoint in each part of the animal experiment, the mice were sacrificed by an overdose of isoflurane,

Table 1. The Molecular Complex Detection (MCODE) Score and Nodes of Clusters.

Cluster	Score	Density	Nodes	Genes
A	7.8	11	39	TSLP, PTX3, ICAMI1, CXCL5, IL18, CXCL8, IGFBP3, IL6, SERPINE1, CXCL3, GDF15
B	3.333	4	5	ASNS, CHAC1, ATF3, TRIB3
C	3	3	3	SCN4A, ANK2, SCN10A

and surgical sides of the hind limb were collected. For HE staining, the tissues were fixed with formalin and embedded with paraffin followed by being cut into 3- μ m-thick sections. We used HE staining to evaluate muscle cell injury scores described as previously reported¹⁶. The proportion of injured muscle cells = injured muscle cells/total number of muscle cells \times 100%. The vessel density in gastrocnemius muscles was measured by CD31 immunohistochemistry. The gastrocnemius muscles were fixed by 4% paraformaldehyde and cut into 3- μ m-thick sections for immunohistochemistry of CD31. CD31 staining was quantified by the ImageJ software.

Preparing the Human Umbilical Vein Endothelial Cells

The human umbilical vein endothelial cells (HUVECs) were purchased from the American Type Culture Collection (ATCC, VA, USA) and cultured in ECM medium with P/S and ECGS under a humidified 5% CO₂ atmosphere at 37°C. To investigate the effect of oxidative stress on SUV39H1 expression on HUVECs, H₂O₂ was added at 100, 200, 300, 400, and 500 μ M into HUVECs for 24 h, respectively. Moreover, to explore whether inhibition of H₂O₂-induced SUV39H1 improved endothelial cell function, the endothelial cell was divided into the H₂O₂ + control siRNA group and the H₂O₂ + SUV39H1 siRNA group. To verify that Sal B and AS-IV could increase angiogenesis through inhibition of SUV39H1 under oxidative stress, the endothelial cell was divided into Sal B/AS-IV + H₂O₂ + vector group and Sal B/AS-IV + H₂O₂ + SUV39H1 plasmid group.

siRNA Transfection

siRNAs (Mission siRNA) against human SUV39H1 and control siRNA were synthesized by GenePharma Biotechnology Co. Ltd. (Shanghai, China). The siRNAs (20 nM) were transiently transfected into HUVECs using HiPerFect Reagent according to the manufacturer's protocol. The siRNA sequences were as follows: Sense 5'-3' GCACAAGUUUGCCUACAAUTT; Antisense 5'-3' AUUGUAGGCAAACUUGUGCTT.

Construction of SUV39H1 Plasmid and Transfection

The SUV39H1 plasmid and empty vector were constructed by the GenePharma Biotechnology Co. Ltd. (Shanghai, China). Briefly, the cells were cultured in 24-well plates for 24 h with 50% confluence. Then, the SUV39H1 plasmid or the empty vector was transfected into cells by lipofectamine 3000 according to the manufacturer's instructions. We used qRT-PCR to detect the transfection efficiency of SUV39H1 after 48 h. The primer sequences are listed in Supplementary Table 1.

Western Blot Analysis

The surgical side of gastrocnemius tissues was used to explore the expression of proteins. Tissues were homogenized by tissue homogenizer (NewZongKe, China) after adding RIPA lysis buffer, PMSF, and protease inhibitor cocktail followed by quantified by the BCA Protein Assay Kit. Next, equal amounts of protein (20–30 μ g) were used for SDS-PAGE electrophoresis and transferred to a PVDF membrane followed by blockage with 5% skim milk for 1 h at room temperature. Then, the membranes were incubated with SUV39H1, Catalase, and GAPDH antibodies at 4°C overnight. After being washed by PBST three times for 10 min, the membranes were incubated with the corresponding secondary antibodies for 1 h followed by three cycles of PBST washing for 10 min each. Finally, the proteins were enhanced with ECL reagent and detected on a UVP BioImaging system (CA, USA).

Quantitative Real-Time PCR Assay

RNAiso was added to the HUVECs to isolate total RNA. PrimeScript RT Master Mix was used to synthesize cDNA followed by qRT-PCR using a Roche SYBR Green PCR Kit. The primers used in this study are listed as follows: (Human) SUV39H1: Sense 5'-3' CCTGCCCTCGGTATCTCTAAG; Antisense 5'-3'

ATATCCACGCCATTTCAACCAG. (Human) GAPDH: Sense 5'-3' GGAGCGAGATCCCTCCAAAAT; Antisense 5'-3' GGCTGTTGTCATACTTCTCATGG.

Tube Formation Assay

The tube formation assay was described as a previous study¹⁷. In brief, each well of a 96-well plate was loaded with 100 μ l of matrigel matrix. Then, HUVECs were seeded on the pre-coated wells at a density of 6×10^4 cells/well. After being cultured for 24 h, images of tube morphology were photographed using an inverted microscope (Leica, DFC290HD, Germany) at \times 100 magnification.

Cell Migration Assay

The cell migration assay was described as a previous study¹⁸. In brief, cells were resuspended and seeded on the upper chambers of the transwell (Corning, MA, USA) and ECM-conditioned medium with 10% fetal bovine serum (FBS) was added to the lower chamber. Then, the migrated cells were fixed with 4% paraformaldehyde and stained with 0.5% crystal violet for 20 min, respectively after 24 h.

Evaluation of Mitochondrial Membrane Potential

Mitochondrial membrane potential (MMP) was detected by the JC-1 probe MMP detection kit according to the manufacturer's instructions. In brief, harvested HUVECs were incubated with the JC-1 detection solution at 37°C for 20 min. The monomeric JC-1 of green fluorescence and the aggregated JC-1 of red fluorescence were visualized by immunofluorescence microscope (DMI6000, Leica, Germany). Fluorescence intensity was quantified using Image J.

Transcriptome Sequencing of siSUV39H1 in HUVECs and Data Mining

After siSUV39H1 was successfully established in HUVECs, the cells were collected for transcriptome sequencing. Sequencing was performed by Ouyi Biotechnology (Shanghai). The differentially expressed genes (DEGs) were further analyzed using the gene ontology (GO) and Kyoto Encyclopedia of Genes and Genomes (KEGG) pathway enrichment analysis.

Protein–Protein Interaction Network Construction and Analysis

The Search Tool for the Retrieval of Interacting Genes/Proteins (STRING) database (<http://string.embl.de/>) was used to assess the associations of DEGs. The PPI network was built and visualized by molecular complex detection (MCODE) in Cytoscape 3.7.2 (<http://cytoscape.org/>), a bioinformatics integration platform. The node centrality analysis was performed in the Cytoscape framework environment using the Hubba plug-in.

Surface Plasmon Resonance

We performed surface plasmon resonance (SPR) on the Biacore T200 system (GE Healthcare Life Sciences, Marlborough, MA, USA). SUV39H1 recombinant protein was diluted with acetate (PH = 4.0) and conjugated to a Series S Sensor Chip CM5 (BR100530, GE Healthcare Life Sciences) by EDC/NHS cross-linking reaction according to manufacturer's protocols. The target immobilization level of SUV39H1 protein was 14,424.8 RU. Sal B and AS-IV were diluted with a

running buffer containing 5% DMSO from 1 to 128 μ M and were injected into the reference channel and SUV39H1 protein channel, respectively, at a flow rate of 30 μ L/min. The coupling time was 60 s and the dissociation time was 120 s. Biacore T200 evaluation software was used to fit the affinity curves by the steady-state affinity model (1:1), and the equilibrium dissociation constant (KD) was calculated.

Molecular Docking of Sal B and AS-IV With SUV39H1

The molecular docking was described in the previous study¹⁹. In brief, the structures of the Sal B and AS-IV were constructed by ChemOffice. Then, MMFF94 force field, RCSB Protein Data Bank, and PyMOL were used to analyze protein structure. Finally, AutoDock and AutoDock Vina were performed for virtual docking.

Statistical Analysis

All of the data are expressed as mean \pm standard deviation (SD) values. Multiple comparisons were performed by one-way analysis of variance (ANOVA) using SPSS 22.0 (SPSS Inc., USA). The *p* values < .05 were considered statistically significant.

Results

SUV39H1 Was Highly Expressed in Mice Ischemic Muscle Tissue

First, we collected the ischemic muscle tissues of mice before the operation, and on Days 4, 8, 12, and 16 after the operation to investigate the expression of SUV39H1 (*n* = 4). The results showed that the blood perfusion of the ischemic limb gradually increased with a decrease in the expression of SUV39H1 (Fig. 1A, B). In contrast, the expression of Catalase in ischemic muscle tissue was increased with the improvement of the blood perfusion of the ischemic limb (Fig. 1C). This result indicated the negative relationships between SUV39H1 and disease outcome.

Chaetocin Protected Against Limb Ischemia in Mice Model

Then, we used chaetocin, a specific inhibitor of SUV39H1, to explore the effect of the inhibition of SUV39H1 on limb ischemia (*n* = 4). The chaetocin-treated model mice exhibited better blood perfusion in the ischemic limb than the Model + DMSO group (Fig. 2A). Moreover, the Model + Chaetocin group showed a higher density of capillaries than the Model + DMSO group (Fig. 2B). The Model + DMSO group had a higher proportion of muscle fiber edema and cell injury. In contrast, muscle fibers in the Model + Chaetocin

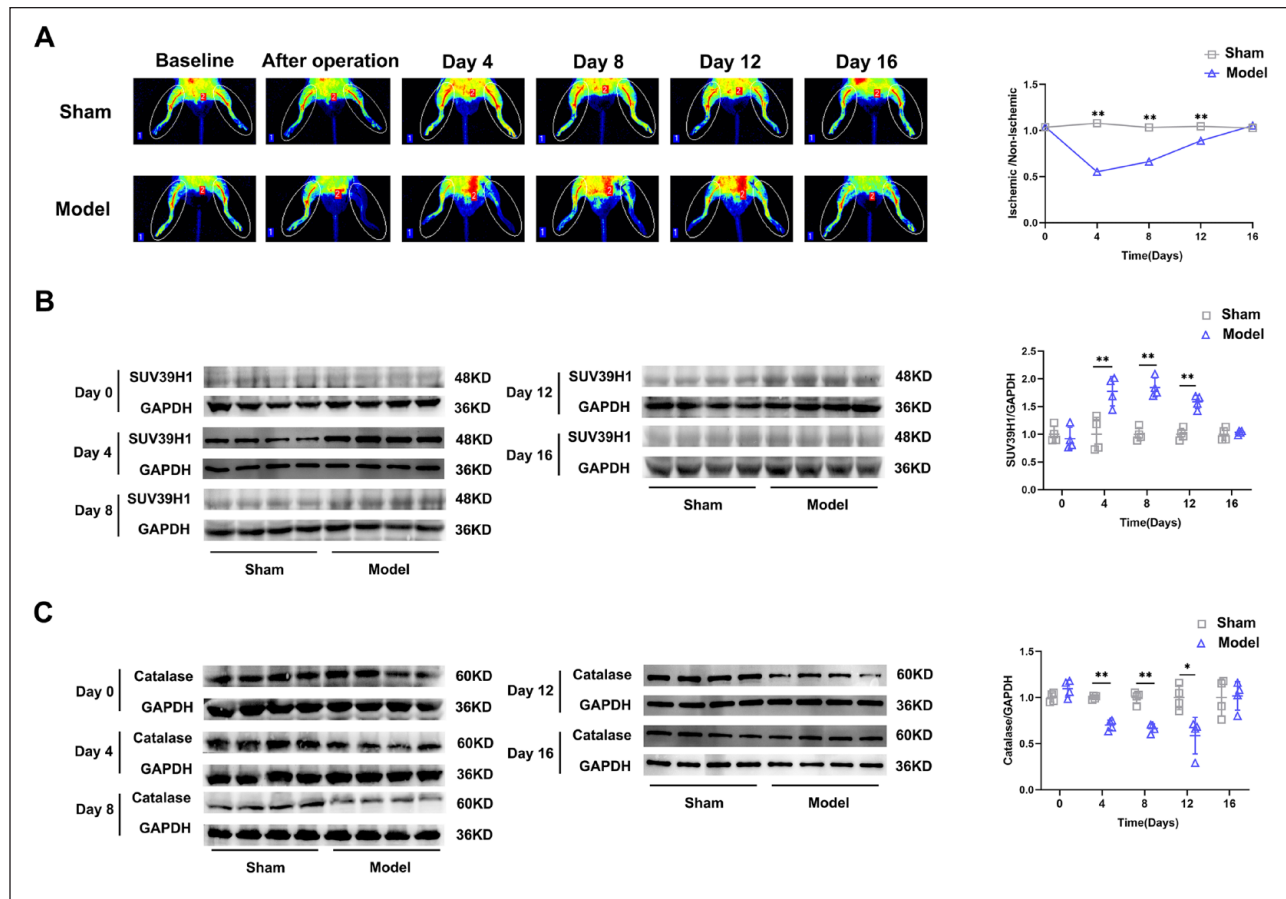


Figure 1. SUV39H1 exhibited higher expression in limb ischemia mice model. (A) Representative photographs of perfusion recovery in ischemic hind limbs before, immediately after, and on Days 4, 8, 12, 14, and 16 after the operation. (B) Protein expression of SUV39H1 in ischemic muscle tissue. (C) Protein expression of Catalase in ischemic muscle tissue (each group $n = 4$; * $P < .05$, ** $P < .01$). GAPDH: glyceraldehyde-3-phosphate dehydrogenase.

group showed rounded and intact borders (Fig. 2C). Furthermore, the expression of SUV39H1 in ischemic muscle tissue was higher in the Model + DMSO group than in the Model + Chaetocin group (Fig. 2D). In contrast, the expression of Catalase in ischemic muscle tissue was higher in the Model + Chaetocin group than in the Model + DMSO group (Fig. 2E). These results suggested that chaetocin increased angiogenesis repair, reduced muscle edema, and reduced oxidative stress through the inhibition of SUV39H1.

SUV39H1 Knockout Improved Limb Ischemia in Mice Model

To further confirm SUV39H1's role in limb ischemia, we constructed an SUV39H1 knockout limb ischemia mice model ($n = 4$). The results showed that SUV39H1 knockout not only promoted blood perfusion (Fig. 3A) but also increased capillary density in the ischemic limb (Fig. 3B). Consistent with chaetocin treatment, SUV39H1 knockout ameliorated muscle fiber injury in ischemic limb muscles (Fig. 3C). Inconsistent with the former results, the

expression of SUV39H1 in ischemic muscle tissue of the WT + Model group was higher than that in WT + Sham group (Fig. 3D). Moreover, the expression of catalase in the ischemic muscle tissue of the SUV39H1 knockout model mice group was higher than in the WT model mice group (Fig. 3E). These results verified that the negative regulation of SUV39H1 on angiogenesis and muscle repair. Moreover, SUV39H1 could regulate oxidative stress response.

SUV39H1 Knockdown Improved H_2O_2 -Induced Endothelial Dysfunction

Considering the level of oxidative stress increased by critical limb ischemia, we found that H_2O_2 up-regulated the expression of SUV39H1 (Fig. 4A). Next, we found better cell migration and tube formation in the H_2O_2 + SUV39H1 siRNA group (Fig. 4B, C). Consistently, SUV39H1 knockdown ameliorated MMP in H_2O_2 + SUV39H1 siRNA group (Fig. 4D). In a word, our results showed that SUV39H1 knockdown promoted cell migration, tube formation, and MMP in endothelial cells under oxidative stress.

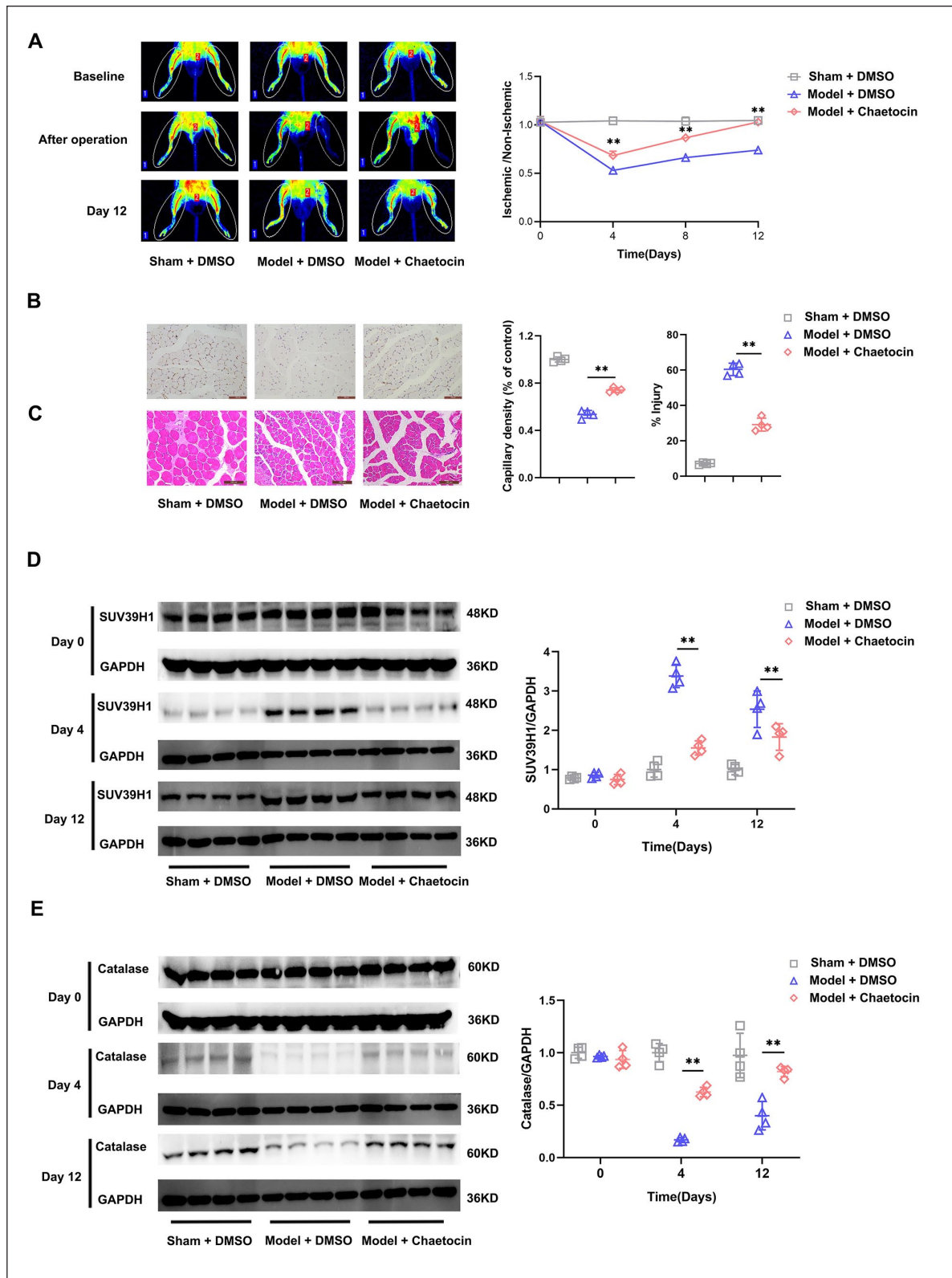


Figure 2. Chaetocin improved limb ischemia in mice model. (A) Representative photographs of perfusion recovery in ischemic hind limbs before, immediately after, and on Days 12 after the operation. (B) Representative photographs of CD31 immunohistochemistry in the ischemic hind limbs. (C) Representative photographs of HE staining in the ischemic hind limbs. (D) Protein expression of SUV39H1 in ischemic muscle tissue. (E) Protein expression of Catalase in ischemic muscle tissue. (Each group $n = 4$; * represents the Model + DMSO group compared with the Model + Chaetocin group; * $P < .05$, ** $P < .01$). DMSO: Dimethyl sulfoxide; GAPDH: glyceraldehyde-3-phosphate dehydrogenase.

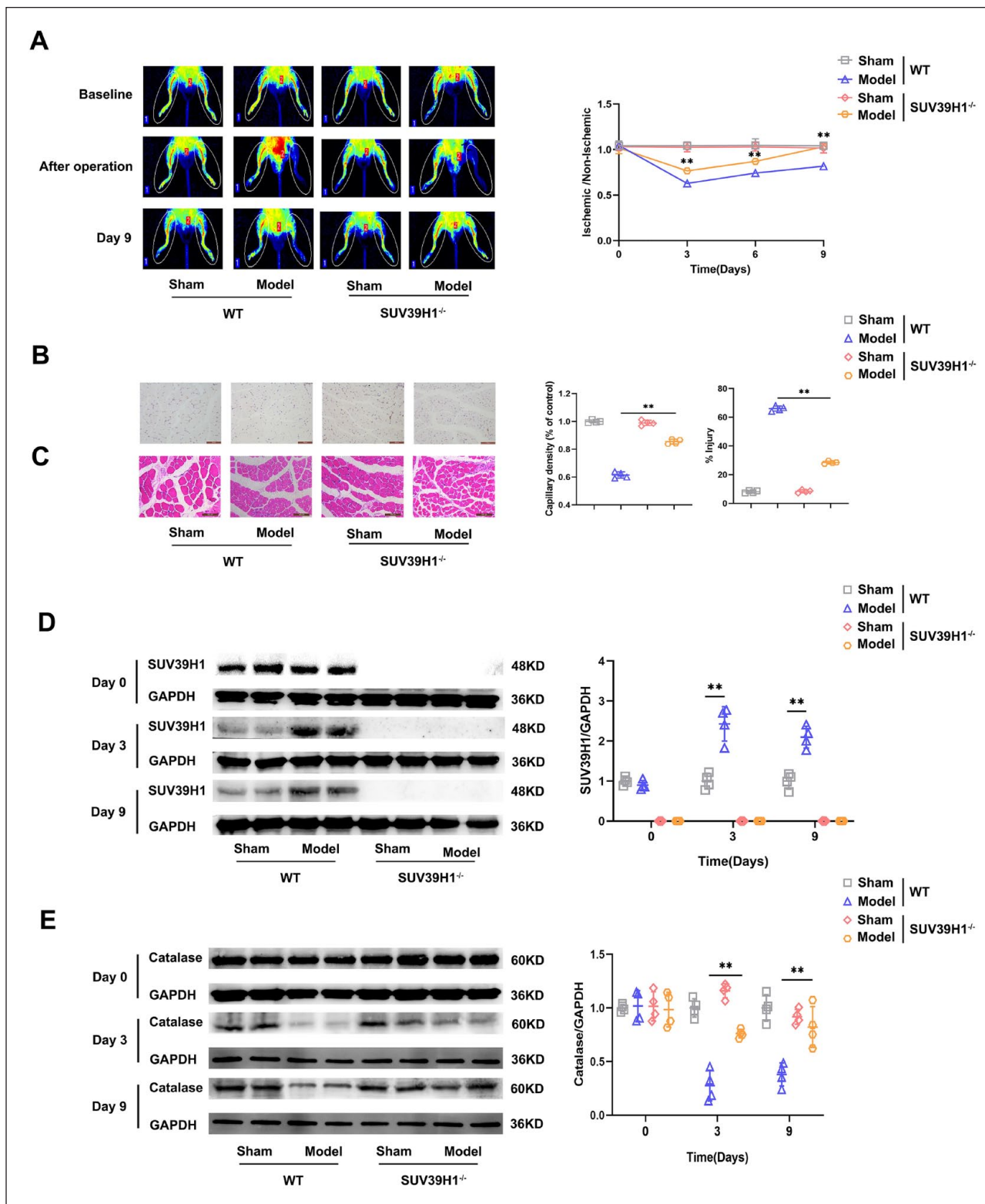


Figure 3. SUV39H1 knockout alleviated limb ischemia in mice model. (A) Representative photographs of perfusion recovery in ischemic hind limbs before, immediately after, and on Days 9 after the operation. (B) Representative photographs of CD31 immunohistochemistry in the ischemic hind limbs. (C) Representative photographs of HE staining in the ischemic hind limbs. (D) Protein expression of SUV39H1 in ischemic muscle tissue. (E) Protein expression of catalase in ischemic muscle tissue. (Each group $n = 4$; * represents the WT + Model group compared with the SUV39H1 knockout + Model group; $*P < .05$, $**P < .01$). GAPDH: glyceraldehyde-3-phosphate dehydrogenase; WT: wild type.

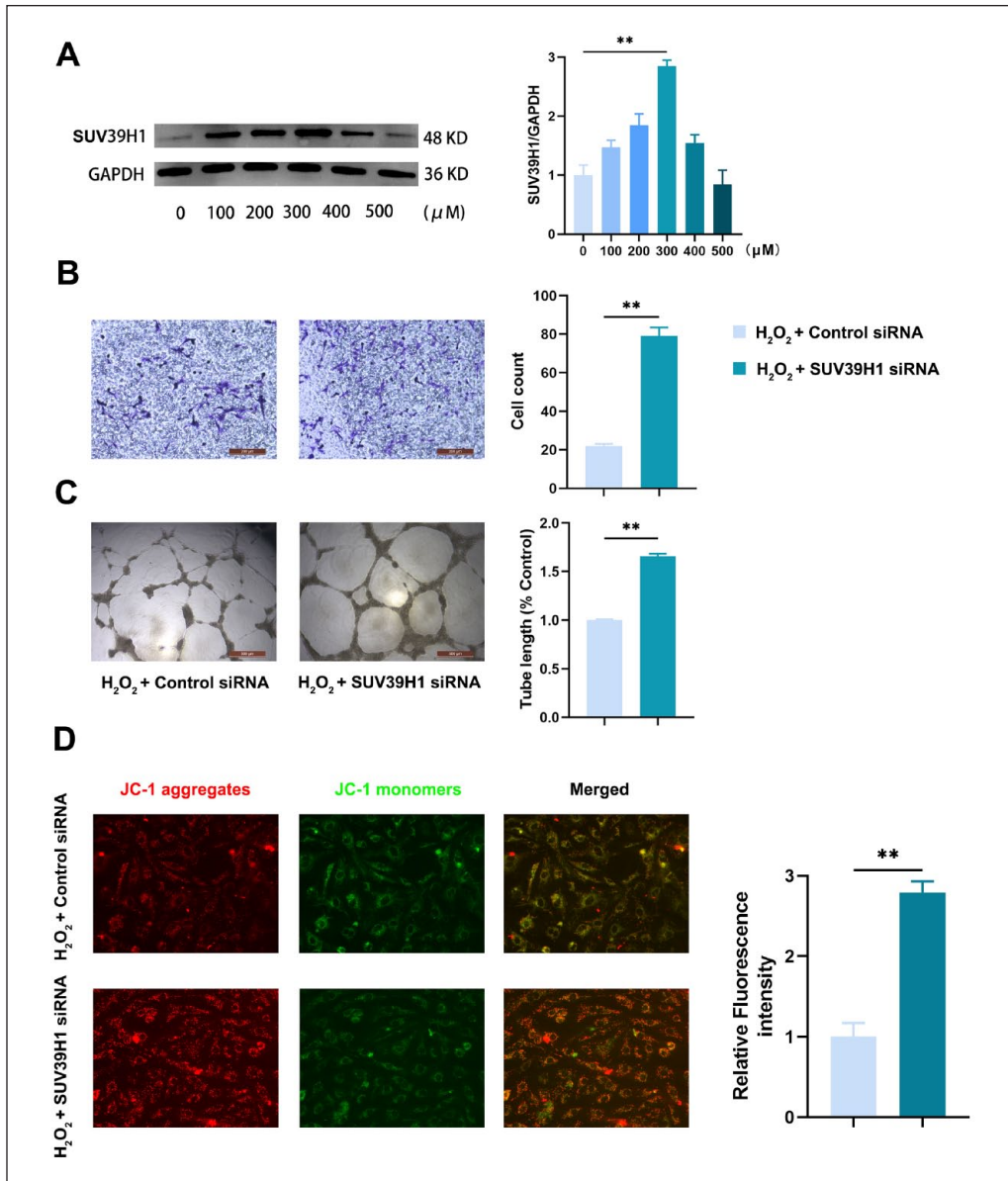


Figure 4. SUV39H1 knockdown improved angiogenesis of HUVECs under oxidative stress. (A) H_2O_2 increased SUV39H1 protein expression in HUVECs. (B) SUV39H1 knockdown increased cell migration in endothelial cells. (C) The ability of tube formation in endothelial cells could be promoted in the SUV39H1 knockdown group. (D) SUV39H1 knockdown improved MMP under oxidative stress in endothelial cells. HUVECs: human umbilical vein endothelial cells; MMP: mitochondrial membrane potential. (* $P < .05$, ** $P < .01$). GAPDH: glyceraldehyde-3-phosphate dehydrogenase; siRNA: Small interfering RNA.

Transcriptome Sequencing of SUV39H1 Knockdown HUVECs

To identify the potential mechanisms caused by SUV39H1 in angiogenesis, we perform transcriptome sequencing (RNA-seq). A total of 14,859 expressed genes in the cell samples. 990 significantly DEGs with Log₂ Fold Change ≥ 1 and P value less than .05 were screened out. Among them, 411 genes were up-regulated and 579 genes were down-regulated (Fig. 5A). Then, the DEGs with twofold or greater changes and a P value less than .01 were screened out and some

high-expression genes were highlighted (Fig. 5A). The heat map generated from differential genes was shown in Fig. 5B.

To explore the underlying mechanisms by which DEGs were involved, these genes were used for the KEGG pathway analysis and GO functional enrichment. In the GO annotation analysis, the DEGs were primarily enriched in diverse biological processes.

The GO-BP were mostly concentrated in the response to extracellular stimulus, regulation of ion transport, cellular response to cytokine stimulus, positive regulation of apoptotic process, and positive regulation of cell death. The GO-CC

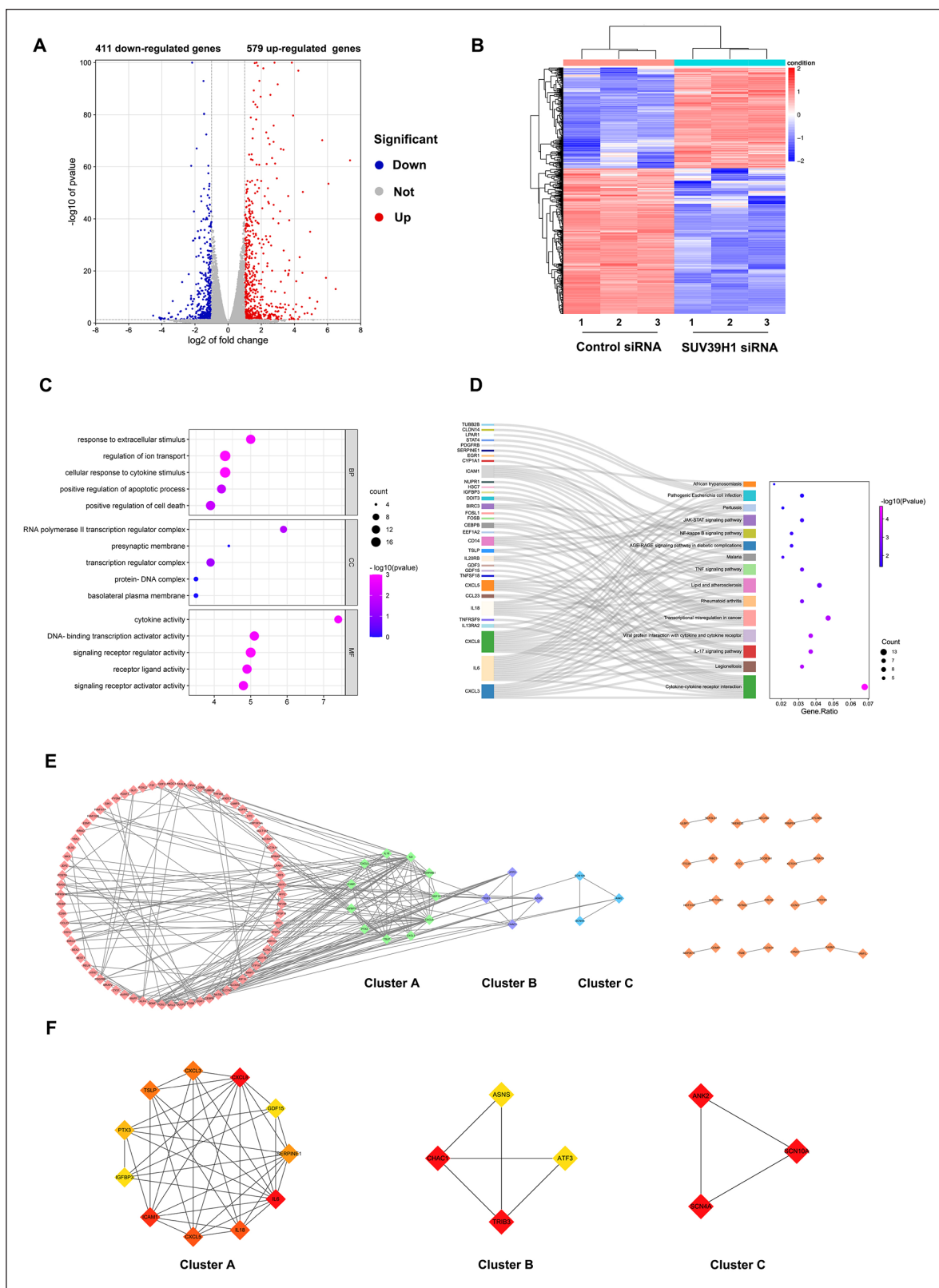


Figure 5. Differential gene expression analysis in SUV39H1 knockdown HUVECs. (A) Volcanic hot spot map of differential expression genes. (B) Gene expression heat map. (C) GO enrichment analysis of DEGs. (D) KEGG pathway enrichment analysis of DEGs. (E) Protein–protein interactions of DEGs, and three modules were identified in DEGs. (F) CytoHubba identified the top hub genes in each module. HUVECs: human umbilical vein endothelial cells; GO: gene ontology; KEGG: Kyoto Encyclopedia of Genes and Genomes; DEGs: differentially expressed genes.

Table 2. Binding Affinity Between SUV39H1 and Compounds.

Compound	Binding affinity (kJ/mol)	Compound	Binding affinity (kJ/mol)
Punicalagin	-7.8	Apigenin	-6.3
Celastrrol	-7.6	Glycoumarin	-6.3
Salvianolic acid B	-7.4	Icariin	-6.3
Berberine	-7.2	Irisin	-6.3
Danshenol A	-6.9	Oroxylin a	-6.3
Luteoloside	-6.9	Atractylenolide III	-6.2
Astragaloside IV	-6.9	Chrysin	-6.2
Tanshinol B	-6.8	Isodeoxyelephantopin	-6.2
Ginsenoside Rg3	-6.7	Obeticholic Acid	-6.2
Silibinin	-6.7	Imperatorin	-6.1
Gambogic acid	-6.6	Salvianolic Acid A	-6.1
Asiatic acid	-6.6	Syringaresinol	-6.1
Puerarin	-6.6	Brevilin A	-6.1
Cyclovirobuxine D	-6.5	Curcumin	-6
Echinacoside	-6.5	Hydroxysafflor Yellow A	-6
Tanshinol A	-6.5	Pterostilbene	-6
Cholic Acid	-6.4	Gastrodin	-5.4
Farrerol	-6.4	Osthol	-5.4
Ginsenoside Rd	-6.4	Caffeic acid	-5.1
Ginsenoside Rg1	-6.4	Protocatechuic acid	-4.5
Paeoniflorin	-6.4	Tetramethylpyrazine	-4
Ginsenoside Rb1	-6.3	Stachydrine	-3.9

were mostly enriched in RNA polymerase II transcription regulator complex, presynaptic membrane, transcription regulator complex, protein-DNA complex, and basolateral plasma membrane. The GO-MF were mostly enriched in cytokine activity, DNA-binding transcription activator activity cytokine activity, signaling receptor regulator activity, receptor-ligand activity, and signaling receptor activator activity. The GO enrichment was represented through a bubble diagram (Fig. 5C). The KEGG pathway enrichment analysis showed that the DEGs were enriched in diverse pathways such as the JAK-STAT signaling pathway, NF-kappa B signaling pathway, tumor necrosis factor (TNF) signaling pathway, and interleukin (IL)-17 signaling pathway (Fig. 5D).

STRING and Cytoscape were used to explore the interaction between hub genes of DEGs and protein-protein interactions (Fig. 5E). MCODE plugin in Cytoscape was used to identify highly interconnected modules (Fig. 5E). The genes, MCODE score, and nodes of every cluster were shown in Table 1. In addition, we used CytoHubba to reveal the top hub genes in each cluster (Fig. 5F).

Sal B and AS-IV Promoted Angiogenesis Through Inhibition of SUV39H1 Under Oxidative Stress

We sought small molecule compounds with proven association with angiogenesis activity through a previous study²⁰.

Then, Sal B and AS-IV were selected as candidate compounds due to good binding energy with SUV39H1 and angiogenesis-promoting ability (Table 2). The results showed that both Sal B and AS-IV could decrease the expression of SUV39H1 (Fig. 6A). Moreover, overexpression of SUV39H1 could attenuate the protective effect of Sal B and AS-IV on angiogenesis and MMP (Fig. 6B, C).

SPR Showed a Good Binding Ability Between AS-IV and SUV39H1 Protein

To validate the interaction of Sal B and AS-IV with SUV39H1 protein, we used SPR to evaluate the interaction at the molecular level. The result showed that AS-IV interacted with recombinant human SUV39H1 (rhSUV39H1) protein with a KD of 0.00002137 M (Fig. 7A). However, we did not obtain the KD between Sal B and SUV39H1. Then, AS-IV-binding sites with SUV39H1 were presented in schematic diagrams (Fig. 7B).

Discussion

In this study, we demonstrate that SUV39H1 aggravated limb ischemia through the inhibition of angiogenesis in mice models. Our experimental data support this conclusion. First, increased expression of SUV39H1 has a relationship with the slow recovery of ischemic limb blood perfusion and angiogenesis. Second, these results are further verified by genetic deletion or pharmaceutical inhibition of SUV39H1 in the ischemic limb mice model. Third, the down-regulation of SUV39H1 was found to be responsible for the improvement in cell migration, tube formation, and MMP in endothelial cells under oxidative stress. PAD has widely been regarded to be a male-dominant disease²¹. The incidence of PAD was 23.05 per 10,000 person-years in males and 12.37 per 10,000 person-years in females²². In Asian countries, such as Korea, male patients accounted for a higher proportion than female patients who received angioplasty²³. Hence, we select male mice in the present experimental work. Current knowledge of the molecular pathways underlying vascular disease in limb ischemia patients is limited. Our study showed a new mechanism for this vascular complication.

The formation of new blood vessels in the ischemic limb is crucial for the improvement of limb ischemia and multiple factors involved in angiogenesis. Among them, excess hydrogen peroxide production in ischemic issues damages the proliferation of endothelial cells, accelerates the apoptosis of endothelial cells, and inhibits the formation of blood vessels^{24,25}. In this study, we found that inhibition of SUV39H1 induced by oxidative stress in vascular endothelial cells can significantly improve angiogenesis, suggesting that SUV39H1 can be a target for PAD treatment. Study on the transplantation of SUV39H1-modified endothelial cells into ischemic tissue is limited. However, in the field of diabetic treatment, HIP (human proislet peptide) could improve

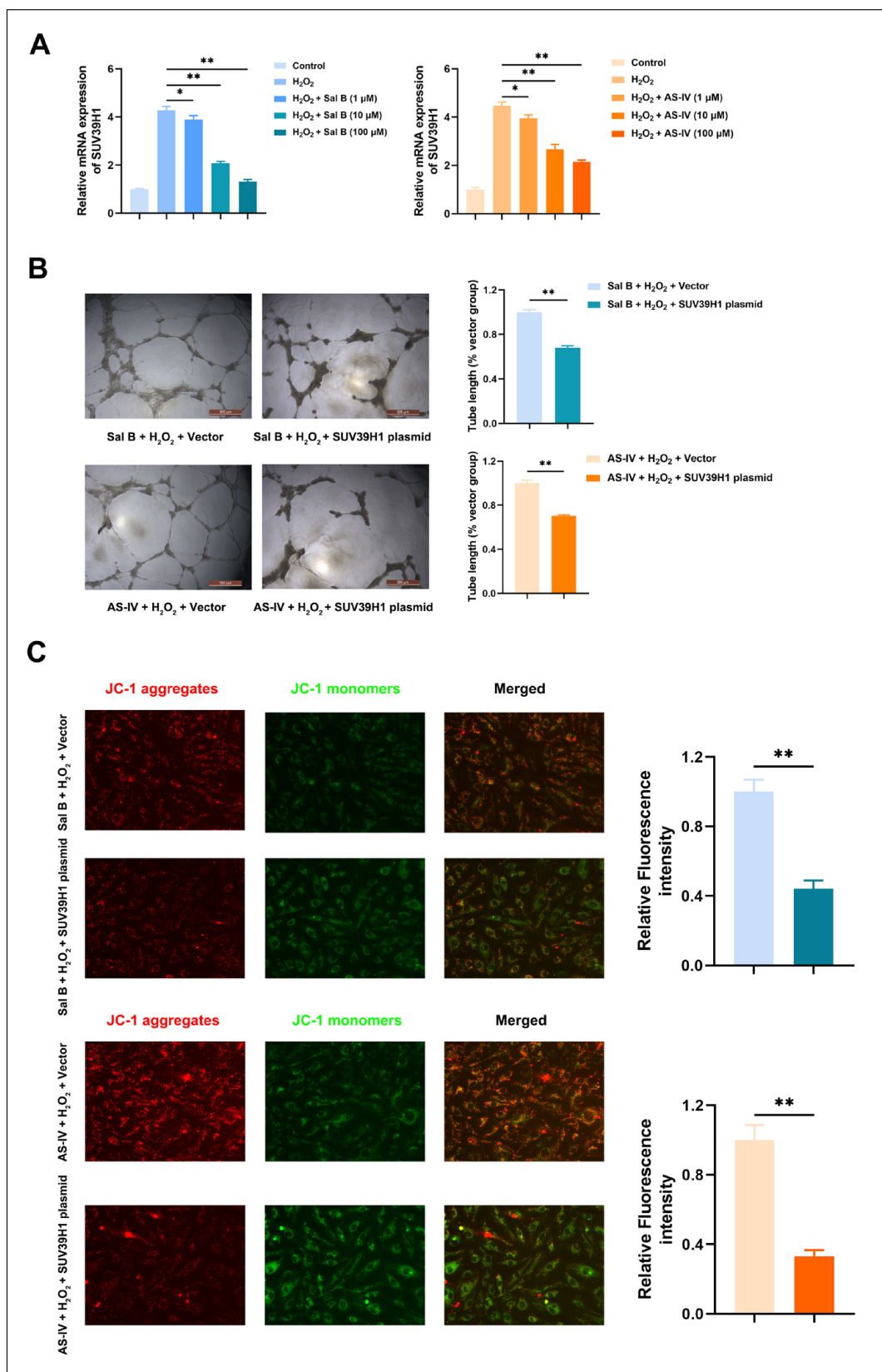


Figure 6. Sal B and AS-IV could promote angiogenesis and MMP through inhibition of SUV39H1 under oxidative stress, respectively. (A) Sal B and AS-IV decreased mRNA expression of SUV39H1 in endothelial cells under oxidative stress, respectively. (B) Overexpression of SUV39H1 attenuated tube formation induced by Sal B and AS-IV, respectively. (C) Overexpression of SUV39H1 attenuated MMP induced by Sal B and AS-IV, respectively. Sal B: Salvianolic acid B; AS-IV: Astragaloside IV; MMP: Mitochondrial Membrane Potential. (**P* < .05, ***P* < .01).

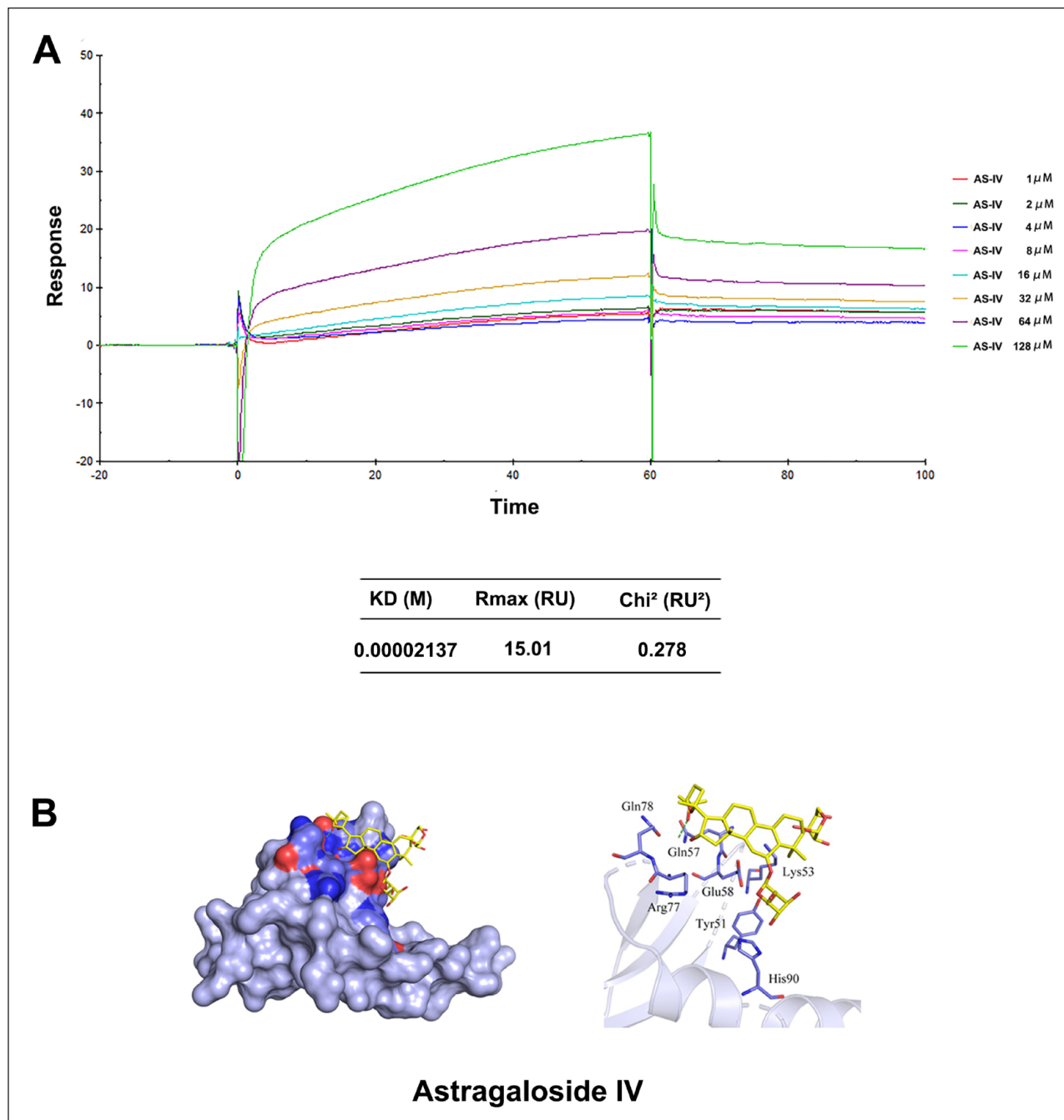


Figure 7. SPR showed a good binding ability between AS-IV and SUV39H1 protein. (A) SPR analysis of direct interaction and binding affinity between AS-IV and recombinant human SUV39H1. (B) Schematic diagrams showed the AS-IV-binding sites with SUV39H1. SPR: Surface Plasmon Resonance; AS-IV: Astragaloside IV.

insulin content and promote the ability of HFPPCs (human fetus-derived pancreatic progenitor cells) to normalize the blood glucose in HFPPCs-transplanted diabetic mice. In terms of the mechanism, HIP could decrease recruitment of H3K9 methyltransferase SUV39H1 and thus reduce repressive H3K9me3 at the promoters of PDX-1, MAFA, and NKX6.1 contributing to the differentiation of pancreatic islets²⁶. Hence, we speculate that hydrogen peroxide-induced

SUV39H1 inhibits blood vessel formation, perhaps by accelerating H3K9me3 at the promoters of angiogenesis-associated genes such as *VEGFA*, *PLGF*, or *HGF*, thus deteriorating the improvement of limb ischemia.

Previous work has shown that SUV39H1 has different roles in different diseases. Sun and colleagues have identified SUV39H-mediated SIRT1 repression as an important mechanism in the progression of myocardial infarction¹³.

Furthermore, regulation of SUV39H1 may ameliorate oxidative stress-induced transcriptional programs and prevent vascular disease in obese people¹⁴. Those works indicate the negative regulatory role of SUV39H1 in disease outcomes. Previous studies also have screened SUV39H-regulated H3K9 trimethylation as an important link between aging and memory loss in mice^{27,28}. Coincidentally, limb ischemia occurs mainly in an elderly population. Given that chaetocin and SUV39H1 knockout improve angiogenesis in limb ischemia of mice, these observations indicate that SUV39H1 could regulate aging-related pathophysiological processes through key transcription events²⁹.

In this study, transcriptome sequencing of siSUV39H1 HUVECs was used to investigating the mechanism involved. In the GO BP annotation analysis, the apoptotic process was involved. SUV39H1 is closely related to apoptosis of tumor cells such as colon carcinoma and glioblastom^{30,31}. Moreover, SUV39H augmented intracellular reactive oxygen species (ROS) levels in a SIRT1-dependent manner, which eventually enlarged infarct size in myocardial infarction¹³. Therefore, pharmacological or genetic regulation of SUV39H1 could be an effective approach to improve disease outcomes. In the KEGG annotation analysis, the JAK-STAT signaling pathway, NF-kappa B signaling pathway, and TNF signaling pathway were enriched. H3K9me3 upregulates the expression and phosphorylation of NF-κB, and in turn, phosphorylated NF-κB increases the expression and phosphorylation of STAT3 under inflammatory conditions³². Furthermore, in caloric restriction of skeletal muscle of male rats, decreased expression of methyltransferase SUV39H1 was followed by decreased TNF promoter and coding region binding of NF-κB³³. In contrast, Ad-SUV39H1 may lead to a decreased activity of the mitogen-activated protein kinase family and its down-stream transcriptional factor NF-κB to protect diabetic rats from myocardial ischemia-reperfusion injury³⁴. We also screened out numerous genes to predict potential mechanisms induced by SUV39H1. SUV39H1 is a histone methyltransferase that specifically methylates lysine 9 of histone H3 and functions as a transcriptional repressor. Previous work has shown that the H3K9me3 had been related to sets of genes involved in angiogenesis and cytoskeletal organization in embryonic fibroblasts from a β-actin knockout mouse³⁵. Moreover, H3K9 histone methylation is involved in cancer invasion and metastasis by promoting cancer angiogenesis³⁶. In addition, epigenetic editing of H3K9 has a relationship with the deregulation of metabolic genes, appetite changes, insulin-signaling defects, and altered expression profile of inflammatory genes³⁷⁻³⁹.

We demonstrate for the first time that the SUV39H1 was confirmed responsible for the slow recovery of ischemic limb blood perfusion and angiogenesis in model mice.

That is to say, regulating SUV39H1 expression may exert a therapeutic effect on angiogenesis in limb ischemia⁴⁰. Hence, based on molecular docking and previous studies, we found Sal B and AS-IV could promote angiogenesis through

inhibition of SUV39H1 under oxidative stress. Sal B extracted from *Salvia miltiorrhiza* prevents patients from ischemic disease via antioxidant and anti-inflammatory properties^{41,42}. Our previous work has shown that Sal B alleviated limb ischemia in mice, SUV39H1 may be involve in this pathophysiological process¹⁹. AS-IV purified from *Astragalus membranaceus* is a common traditional Chinese medicine (TCM) for the treatment of cardiovascular and cerebrovascular ischemia^{43,44}. It also depresses the level of intracellular oxidative stress via the activities of antioxidant enzymes such as glutathione peroxidase (GSH-Px) and superoxide dismutase (SOD)⁴⁵. Hence, Sal B and AS-IV could be potential drug candidates for limb ischemia.

In the present, we showed that the slow recovery of ischemic limb blood perfusion and angiogenesis in experimental mice were associated with SUV39H1. The genetic deletion or pharmaceutical inhibition of SUV39H1 ameliorated muscle injury and promoted angiogenesis, which eventually improved limb ischemia. However, our study still has limitations. First, more oxidative stress-related markers should be tested to confirm the relationship between SUV39H1 and oxidative stress. Second, the signaling pathways should be tested to verify the potential mechanism involved in SUV39H1-related angiogenesis.

Conclusion

In summary, our data demonstrate the potential of SUV39H1 deletion/inhibition in alleviating muscle damage and improving angiogenesis associated with limb ischemia. A genome-wide search for potential mechanisms, using transcriptome sequencing, in HUVECs would hopefully clear the interaction between SUV39H1 and angiogenesis.

Author Contributions

W.N. and W.C. designed the study and have contributed equally to this work. W.N. and F.W. analyzed data. W.N. wrote this study. C.L. revised this manuscript.

Data Availability

All data included in this study are available upon request by contacting the corresponding author.

Ethical Approval

This study was approved by our institutional review board.

Statement of Human and Animal Rights

This article does not contain any studies with human or animal subjects.

Statement of Informed Consent

There are no human subjects in this article and informed consent is not applicable.


Declaration of Conflicting Interests

The author(s) declared no potential conflicts of interest with respect to the research, authorship, and/or publication of this article.

Funding

The author(s) disclosed receipt of the following financial support for the research, authorship, and/or publication of this article: This work was supported by the Program of Shanghai Academic Research Leader (grant no. 17XD1405000) awarded to C.L.

ORCID iD

Chun Liang  <https://orcid.org/0000-0002-4042-206X>

Supplemental Material

Supplemental material for this article is available online.

References

- Criqui MH, Aboyans V. Epidemiology of peripheral artery disease. *Circ Res*. 2015;116(9): 1509–26.
- Savji N, Rockman CB, Skolnick AH, Guo Y, Adelman MA, Riles T, Berger JS. Association between advanced age and vascular disease in different arterial territories: a population database of over 3.6 million subjects. *J Am Coll Cardiol*. 2013;61(16): 1736–43.
- Ostchega Y, Paulose-Ram R, Dillon CF, Gu Q, Hughes JP. Prevalence of peripheral arterial disease and risk factors in persons aged 60 and older: data from the National Health and Nutrition Examination Survey 1999–2004. *J Am Geriatr Soc*. 2007;55(4): 583–89.
- Tsao CW, Aday AW, Almarzooq ZI, Alonso A, Beaton AZ, Bittencourt MS, Boehme AK, Buxton AE, Carson AP, Commodore-Mensah Y, Elkind MSV, et al. Heart Disease and stroke statistics–2022 update: a report from the American Heart Association. *Circulation*. 2022;145(8): e153–e639.
- Yu H, He J, Liu W, Feng S, Gao L, Xu Y, Zhang Y, Hou X, Zhou Y, Yang L, Wang X. The transcriptional coactivator, ALL1-fused gene from chromosome 9, simultaneously sustains hypoxia tolerance and metabolic advantages in liver cancer. *Hepatology*. 2021;74(4): 1952–70.
- Bárcena-Varela M, Caruso S, Llerena S, Álvarez-Sola G, Uriarte I, Latasa MU, Urtasun R, Rebouissou S, Alvarez L, Jimenez M, Santamaría E, et al. Dual targeting of histone methyltransferase G9a and DNA-methyltransferase 1 for the treatment of experimental hepatocellular carcinoma. *Hepatology*. 2019;69(2): 587–603.
- Hamdani N, Costantino S, Mugge A, Lebeche D, Tschöpe C, Thum T, Paneni F. Leveraging clinical epigenetics in heart failure with preserved ejection fraction: a call for individualized therapies. *Eur Heart J*. 2021;42(20): 1940–58.
- Abdelmegeed MA, Banerjee A, Yoo SH, Jang S, Gonzalez FJ, Song BJ. Critical role of cytochrome P450 2E1 (CYP2E1) in the development of high fat-induced non-alcoholic steatohepatitis. *J Hepatol*. 2012;57(4): 860–66.
- Xu S, Kamato D, Little PJ, Nakagawa S, Pelisek J, Jin ZG. Targeting epigenetics and non-coding RNAs in atherosclerosis: from mechanisms to therapeutics. *Pharmacol Ther*. 2019;196:15–43.
- Ohtani K, Vlachojannis GJ, Koyanagi M, Boeckel JN, Urbich C, Farcas R, Bonig H, Marquez VE, Zeiher AM, Dimmeler S. Epigenetic regulation of endothelial lineage committed genes in pro-angiogenic hematopoietic and endothelial progenitor cells. *Circ Res*. 2011;109(11): 1219–29.
- Wang K, Li Y, Qiang T, Chen J, Wang X. Role of epigenetic regulation in myocardial ischemia/reperfusion injury. *Pharmacol Res*. 2021;170:105743.
- Liu H, Wang W, Weng X, Chen H, Chen Z, Du Y, Liu X, Wang L. The H3K9 histone methyltransferase G9a modulates renal ischemia reperfusion injury by targeting Sirt1. *Free Radic Biol Med*. 2021;172:123–35.
- Yang G, Weng X, Zhao Y, Zhang X, Hu Y, Dai X, Liang P, Wang P, Ma L, Sun X, Hou L, et al. The histone H3K9 methyltransferase SUV39H links SIRT1 repression to myocardial infarction. *Nat Commun*. 2017;8:14941.
- Costantino S, Paneni F, Virdis A, Hussain S, Mohammed SA, Capretti G, Akhmedov A, Dalgaard K, Chiandotto S, Pospisilik JA, Jenuwein T. Interplay among H3K9-editing enzymes SUV39H1, JMJD2C and SRC-1 drives p66Shc transcription and vascular oxidative stress in obesity. *Eur Heart J*. 2019;40(4): 383–91.
- Limbourg A, Korff T, Napp LC, Schaper W, Drexler H, Limbourg FP. Evaluation of postnatal arteriogenesis and angiogenesis in a mouse model of hind-limb ischemia. *Nat Protoc*. 2009;4(12): 1737–46.
- Chen Y, Niu W, Chao YC, He Z, Ding R, Wu F, Liang C. Alagebrium targets the miR-27b/TSP-1 signaling pathway to rescue N-carboxymethyl-lysine-induced endothelial dysfunction. *Am J Transl Res*. 2019;11(3): 1569–80.
- Hamada H, Kim MK, Iwakura A, Ii M, Thorne T, Qin G, Asai J, Tsutsumi Y, Sekiguchi H, Silver M, Wecker A, et al. Estrogen receptors alpha and beta mediate contribution of bone marrow-derived endothelial progenitor cells to functional recovery after myocardial infarction. *Circulation*. 2006;114(21): 2261–70.
- Li Y, Ren Y, Wang Y, Tan Y, Wang Q, Cai J, Zhou J, Yang C, Zhao K, Yi K, Jin W, et al. A compound AC1Q3QWB selectively disrupts HOTAIR-mediated recruitment of PRC2 and enhances cancer therapy of DZNep. *Theranostics*. 2019;9(16): 4608–23.
- Niu W, Wu F, Cao W, Chen Y, Zhang Y, Chen Y, Ding R, Liang C. Salvianolic acid B alleviates limb ischemia in mice via promoting SIRT1/PI3K/AKT pathway-mediated M2 macrophage polarization. *Evid Based Complement Alternat Med*. 2022;2022:1112394.
- Bu L, Dai O, Zhou F, Liu F, Chen JF, Peng C, Xiong L. Traditional Chinese medicine formulas, extracts, and compounds promote angiogenesis. *Biomed Pharmacother*. 2020;132: 110855.
- Schramm K, Rochon PJ. Gender differences in peripheral vascular disease. *Semin Intervent Radiol*. 2018;35(1): 9–16.
- Cea-Soriano L, Fowkes FGR, Johansson S, Allum AM, Garcia Rodriguez LA. Time trends in peripheral artery disease incidence, prevalence and secondary preventive therapy: a cohort study in the Health Improvement Network in the UK. *BMJ Open*. 2018;8(1): e018184.
- Ko YG, Ahn CM, Min PK, Lee JH, Yoon CH, Yu CW, Lee SW, Lee SR, Choi SH, Koh YS, Chae IH, et al. Baseline characteristics of a retrospective patient cohort in the Korean Vascular Intervention Society Endovascular Therapy in Lower

- Limb Artery Diseases (K-VIS ELLA) Registry. *Korean Circ J*. 2017;47(4): 469–76.
24. Wen W, Yang L, Wang X, Zhang H, Wu F, Xu K, Chen S, Liao Z. Fucoidan promotes angiogenesis | accelerates wound healing through AKT/Nrf2/HIF-1alpha signalling pathway. *Int Wound J*. Published online May 18, 2023. doi: 10.1111/iwj.14239
 25. Ho YJ, Hsu HC, Wu BH, Lin YC, Liao LD, Yeh CK. Preventing ischemia-reperfusion injury by acousto-mechanical local oxygen delivery. *J Control Release*. 2023;356: 481–92.
 26. Jiang Z, Shi D, Tu Y, Tian J, Zhang W, Xing B, Wang J, Liu S, Lou J, Gustafsson JÅ, Hua X, et al. Human proislet peptide promotes pancreatic progenitor cells to ameliorate diabetes through FOXO1/menin-mediated epigenetic regulation. *Diabetes*. 2018;67(7): 1345–55.
 27. Kushwaha A, Thakur MK. Increase in hippocampal histone H3K9me3 is negatively correlated with memory in old male mice. *BioGerontology*. 2020;21(2): 175–89.
 28. Snigdha S, Prieto GA, Petrosyan A, Loertscher BM, Dieskau AP, Overman LE, Cotman CW. H3K9me3 inhibition improves memory, promotes spine formation, and increases BDNF levels in the aged hippocampus. *J Neurosci*. 2016;36(12): 3611–22.
 29. Liu B, Wang Z, Zhang L, Ghosh S, Zheng H, Zhou Z. Depleting the methyltransferase Suv39h1 improves DNA repair and extends lifespan in a progeria mouse model. *Nat Commun*. 2013;4:1868.
 30. Lu C, Klement JD, Yang D, Albers T, Lebedeva IO, Waller JL, Liu K. SUV39H1 regulates human colon carcinoma apoptosis and cell cycle to promote tumor growth. *Cancer Lett*. 2020;476:87–96.
 31. Ozyerli-Goknar E, Sur-Erdem I, Seker F, Cingoz A, Kayabolen A, Kahya-Yesil Z, Uyulur F, Gezen M, Tolay N, Erman B, Gönen M, et al. The fungal metabolite chaetocin is a sensitizer for pro-apoptotic therapies in glioblastoma. *Cell Death Dis*. 2019;10(12): 894.
 32. Zheng Q, Lin Z, Li X, Xin X, Wu M, An J, Gui X, Li T, Pu H, Li H, Lu D. Inflammatory cytokine IL6 cooperates with CUDR to aggravate hepatocyte-like stem cells malignant transformation through NF-kappaB signaling. *Sci Rep*. 2016;6:36843.
 33. Hernández-Saavedra D, Moody L, Tang X, Goldberg ZJ, Wang AP, Chen H, Pan YX. Caloric restriction following early-life high fat-diet feeding represses skeletal muscle TNF in male rats. *J Nutr Biochem*. 2021;91:108598.
 34. Yang B, Yang J, Bai J, Pu P, Liu J, Wang F, Ruan B. Suv39h1 protects from myocardial ischemia-reperfusion injury in diabetic rats. *Cell Physiol Biochem*. 2014;33(4): 1176–85.
 35. Xie X, Almuzzaini B, Drou N, Kremb S, Yousif A, Farrants AO, Gunsalus K, Percipalle P. Beta-Actin-dependent global chromatin organization and gene expression programs control cellular identity. *FASEB J*. 2018;32(3): 1296–314.
 36. Chen RJ, Shun CT, Yen ML, Chou CH, Lin MC. Methyltransferase G9a promotes cervical cancer angiogenesis and decreases patient survival. *Oncotarget*. 2017;8(37): 62081–98.
 37. Tateishi K, Okada Y, Kallin EM, Zhang Y. Role of Jhd2a in regulating metabolic gene expression and obesity resistance. *Nature*. 2009;458(7239): 757–61.
 38. Zhong L, D'Urso A, Toiber D, Sebastian C, Henry RE, Vadysirisack DD, Guimaraes A, Marinelli B, Wikstrom JD, Nir T, Clish CB, et al. The histone deacetylase Sirt6 regulates glucose homeostasis via Hif1alpha. *Cell*. 2010;140(2): 280–93.
 39. Brasacchio D, Okabe J, Tikellis C, Balcerzyk A, George P, Baker EK, Calkin AC, Brownlee M, Cooper ME, El-Osta A. Hyperglycemia induces a dynamic cooperativity of histone methylase and demethylase enzymes associated with gene-activating epigenetic marks that coexist on the lysine tail. *Diabetes*. 2009;58(5): 1229–36.
 40. Napoli C, Crudele V, Soricelli A, Al-Omran M, Vitale N, Infante T, Mancini FP. Primary prevention of atherosclerosis: a clinical challenge for the reversal of epigenetic mechanisms? *Circulation*. 2012;125(19): 2363–73.
 41. Luo J, Zhang L, Zhang X, Long Y, Zou F, Yan C, Zou W. Protective effects and active ingredients of *Salvia miltiorrhiza* Bunge extracts on airway responsiveness, inflammation and remodeling in mice with ovalbumin-induced allergic asthma. *Phytomedicine*. 2019;52:168–77.
 42. Luo Y, Fan C, Yang M, Dong M, Bucala R, Pei Z, Zhang Y, Ren J. CD74 knockout protects against LPS-induced myocardial contractile dysfunction through AMPK-Skp2-SUV39H1-mediated demethylation of BCLB. *Br J Pharmacol*. 2020;177(8): 1881–97.
 43. Lu Y, Li S, Wu H, Bian Z, Xu J, Gu C, Chen X, Yang D. Beneficial effects of astragaloside IV against angiotensin II-induced mitochondrial dysfunction in rat vascular smooth muscle cells. *Int J Mol Med*. 2015;36(5): 1223–32.
 44. Chiu BY, Chang CP, Lin JW, Yu JS, Liu WP, Hsu YC, Lin MT. Beneficial effect of astragalosides on stroke condition using PC12 cells under oxygen glucose deprivation and reperfusion. *Cell Mol Neurobiol*. 2014;34(6): 825–37.
 45. Li L, Hou X, Xu R, Liu C, Tu M. Research review on the pharmacological effects of astragaloside IV. *Fundam Clin Pharmacol*. 2017;31(1): 17–36.